

## The effect of composite resonances on EWPT and Higgs decay into two photons

A. E. CÁRCAMO HERNÁNDEZ(\*), C. O. DIB(\*\*) and A. R. ZERWEKH(\*\*\*)

*Universidad Técnica Federico Santa María and Centro Científico-Tecnológico de Valparaíso  
Casilla 110-V, Valparaíso, Chile*

ricevuto 20 Giugno 2013

**Summary.** — In the context of strongly coupled electroweak symmetry breaking, heavy composite particles of different spin and parity may arise and cause observable effects at loop levels. We use an effective chiral Lagrangian to describe the interactions amongst these composite resonances and the SM fields. We study the effects of the composite particles on the Higgs decay into two photons and on the oblique  $T$  and  $S$  parameters. Consistency with the  $T$  and  $S$  parameters and the newly observed Higgs decay into  $\gamma\gamma$  can be found, for axial vector masses in the range  $1.7 \text{ TeV} \lesssim M_A \lesssim 2 \text{ TeV}$  and vector masses  $\sim 0.8M_A$ , provided a non-standard kinetic mixing between the  $W^3$  and  $B^0$  fields is included.

PACS 11.10.-z – Field theory.

### 1. – Introduction

The ATLAS and CMS experiments at the CERN Large Hadron Collider (LHC) have found signals consistent with a  $\sim 126 \text{ GeV}$  Higgs boson [1-3]. This discovery offers the possibility to unveil the mechanism of Electroweak Symmetry Breaking (EWSB). Still pending in the LHC studies is to establish the quantum numbers of this particle and to measure its couplings to the standard fermions and gauge bosons. In particular, it is important to determine whether the new observed state comes from a weakly or strongly coupled dynamics. Examples of weakly coupled scenarios of EWSB are the original Higgs sector of the Standard Model, Multi Higgs Models or their Supersymmetric extensions. Alternatively, strong scenarios correspond to composite models such as technicolor theories in their several versions. The current theory of strong and electroweak interactions,

(\*) E-mail: antonio.carcamo@usm.cl

(\*\*) E-mail: claudio.dib@usm.cl

(\*\*\*) E-mail: alfonso.zerwekh@usm.cl

the Standard Model (SM), has proven to be remarkably consistent with all experimental tests, including high precision measurements [4]. However, there are reasons to believe that the SM is only a low energy effective framework of a yet unknown more fundamental theory. One of them is the hierarchy problem, which indicates that new physics should appear at scales not much higher than the EWSB scale (say, around a few TeV) in order to stabilize the Higgs mass at scales much lower than the Planck scale ( $\sim 10^{19}$  GeV).

A possible scenario that solves this problem is that of a strongly interacting dynamics without fundamental scalars that becomes non-perturbative somewhere above the EW scale, causing the breakdown of the electroweak symmetry through the formation of condensates in the vacuum. In the strongly interacting picture of EWSB, many models have been proposed, which predict the existence of composite particles such as composite scalars [5-12], composite vectors [13-15], composite scalars and vectors [16-20] and composite fermions [21, 22]. These predicted scalar and vector resonances play a very important role in preserving the unitarity of longitudinal gauge boson scattering up to the cutoff  $\Lambda \simeq 4\pi v$ . One should add that a composite scalar does not have the hierarchy problem since quantum corrections to its mass are saturated at the compositeness scale, which is assumed to be much lower than the Planck scale.

In this work we assume a scenario where there is a strongly interacting sector which possesses a global  $SU(2)_L \times SU(2)_R$  symmetry. The strong dynamics responsible for EWSB, in general gives rise to massive composite vector and axial vector fields ( $V_\mu^a$  and  $A_\mu^a$ , respectively) belonging to the triplet representation of the  $SU(2)_{L+R}$  custodial group, as well as two massive composite scalars ( $h$  and  $H$ ) and one pseudoscalar ( $\eta$ ) all singlets under that group. We will identify the lightest scalar,  $h$ , with the state of mass  $m_h = 126$  GeV discovered at the LHC. All of these composite resonances are assumed to be lighter than the cutoff  $\Lambda \simeq 4\pi v$ , so that they explicitly appear as fields in the effective chiral Lagrangian. In this work we use the high precision results on  $S$  and  $T$  to constrain the mass and coupling parameters of the model, and then study the rates of  $h \rightarrow \gamma\gamma$  which are consistent with the previous constraints and at the same time can explain the recently observed excess of this channel at the LHC.

## 2. – The model

The Lagrangian of our effective theory is given by [20]

$$\begin{aligned}
(1) \quad \mathcal{L} = & \frac{v^2}{4} \langle D_\mu U D^\mu U^\dagger \rangle - \frac{1}{2g^2} \langle W_{\mu\nu} W^{\mu\nu} \rangle - \frac{1}{2g'^2} \langle B_{\mu\nu} B^{\mu\nu} \rangle + \frac{c_{WB}}{4} \langle U^\dagger W_{\mu\nu} U B^{\mu\nu} \rangle \\
& + \sum_{R=V,A} \left[ -\frac{1}{4} \langle R_{\mu\nu} R^{\mu\nu} \rangle + \frac{1}{2} M_R^2 R_\mu R^\mu \right] - \frac{f_V}{2\sqrt{2}} \langle V^{\mu\nu} (u W_{\mu\nu} u^\dagger + u^\dagger B_{\mu\nu} u) \rangle \\
& - \frac{ig_V}{2\sqrt{2}} \langle V^{\mu\nu} [u_\mu, u_\nu] \rangle + \frac{f_A}{2\sqrt{2}} \langle u_{\mu\nu} A^{\mu\nu} \rangle - \frac{if_A}{2\sqrt{2}} \langle (u W_{\mu\nu} u^\dagger + u^\dagger B_{\mu\nu} u) [A^\mu, u^\nu] \rangle \\
& - \frac{i\kappa f_A}{2\sqrt{2}} \langle u_{\mu\nu} [V^\mu, u^\nu] \rangle + \sum_{S=h,H,\eta} \left[ \frac{1}{2} \partial_\mu S \partial^\mu S + \frac{m_S^2}{2} S^2 \right] \\
& + \alpha_\eta \langle V_\mu A^\mu \rangle \eta + \beta_\eta \langle V_\mu u^\mu \rangle \eta \\
& + \sum_{S=h,H} [\alpha_S S \langle u_\mu u^\mu \rangle + \beta_S S \langle V_\mu V^\mu \rangle + \gamma_S S \langle A_\mu A^\mu \rangle + \delta_S S \langle A_\mu u^\mu \rangle] + \mathcal{L}',
\end{aligned}$$

where  $\mathcal{L}'$  corresponds to the part of the Lagrangian which includes: the interactions of *two* of the heavy spin-one fields with the SM Goldstone bosons and gauge fields, the interactions involving *three* heavy spin-one fields, the quartic self-interactions of  $V_\mu$  and of  $A_\mu$ , the contact interactions involving the SM gauge fields and Goldstone bosons, the interaction terms that include two of the spin-zero fields coupled to the SM Goldstone bosons or gauge fields, or to the composite  $V_\mu$  and  $A_\mu$  fields, the mass terms for the SM quarks as well as interactions between the light Higgs field  $h$  and the SM fermions.

The explicit terms shown in eq. (1) are: kinetic and mass terms for the  $W, B, V, A, h, H$  and  $\eta$  fields,  $W^3$ - $B^0$  kinetic mixing terms, interaction terms linear in the fields  $V, A, h, H$  and  $\eta$ , interaction terms of the form  $SVV, SAA$  ( $S = 3Dh, H$ ) and  $\eta VA$ . Those explicit terms are up to first order in the  $f_V, f_A$  and  $g_V$  couplings.

Besides that, the dimensionless couplings in eq. (1) are given in ref. [20], and the following definitions are fulfilled:

$$\begin{aligned} U(x) &= e^{i\hat{\pi}(x)/v}, & \hat{\pi}(x) &= \tau^a \pi^a, & u &\equiv \sqrt{U}, & B_\mu &= \frac{g'}{2} \tau^3 B_\mu^0, \\ D_\mu U &= \partial_\mu U - iB_\mu U + iUW_\mu, & W_\mu &= \frac{g}{2} \tau^a W_\mu^a, & R_\mu &= \frac{1}{\sqrt{2}} \tau^a R_\mu^a, \\ R &= V, A, & \hat{X}_{\mu\nu} &= \nabla_\mu X_\nu - \nabla_\nu X_\mu, & X &= R, u & u_\mu &= iu^\dagger D_\mu U u^\dagger, \\ \nabla_\mu R &= \partial_\mu R + [\Gamma_\mu, R], & \Gamma_\mu &= \frac{1}{2} \left[ u^\dagger (\partial_\mu - iB_\mu) u + u (\partial_\mu - iW_\mu) u^\dagger \right]. \end{aligned}$$

Our effective theory is based on the following assumptions:

1. The Lagrangian responsible for EWSB has an underlying strong dynamics with a global  $SU(2)_L \times SU(2)_R$  symmetry which is spontaneously broken by the strong dynamics down to the  $SU(2)_{L+R}$  custodial group. The SM electroweak gauge symmetry  $SU(2)_L \times U(1)_Y$  is assumed to be embedded as a local part of the  $SU(2)_L \times SU(2)_R$  symmetry. Thus the spontaneous breaking of  $SU(2)_L \times SU(2)_R$  also leads to the breaking of the electroweak gauge symmetry down to  $U(1)_{em}$ .
2. The strong dynamics produces composite heavy vector fields  $V_\mu^a$  and axial vector fields  $A_\mu^a$ , triplets under the custodial  $SU(2)_{L+R}$ , as well as a composite scalar singlet  $h$  with mass  $m_h = 126$  GeV, a heavier scalar singlet  $H$ , and a heavier pseudoscalar singlet  $\eta$ . These fields are assumed to be the only composites lighter than the symmetry breaking cutoff  $\Lambda \simeq 4\pi v$ .
3. The heavy fields  $V_\mu^a$  and  $A_\mu^a$  couple to SM fermions only through their kinetic mixings with the SM Gauge bosons.
4. The lighter scalar singlet  $h$  interacts with the fermions only via (proto)-Yukawa couplings. The heavy scalar  $H$  and pseudoscalar  $\eta$  are fermiofobic.

### 3. – Numerical study of effects on $T, S$ and $h \rightarrow \gamma\gamma$

In the Standard Model, the  $h \rightarrow \gamma\gamma$  decay is dominated by  $W$  loop diagrams which can interfere destructively with the subdominant top quark loop. In our strongly coupled model, the  $h \rightarrow \gamma\gamma$  decay receives extra contributions from loops with charged  $V_\mu$  and  $A_\mu$ , as shown in fig. 1. In this work we want to determine the range of the heavy vector masses which is consistent with the events in the  $h \rightarrow \gamma\gamma$  decay recently observed at

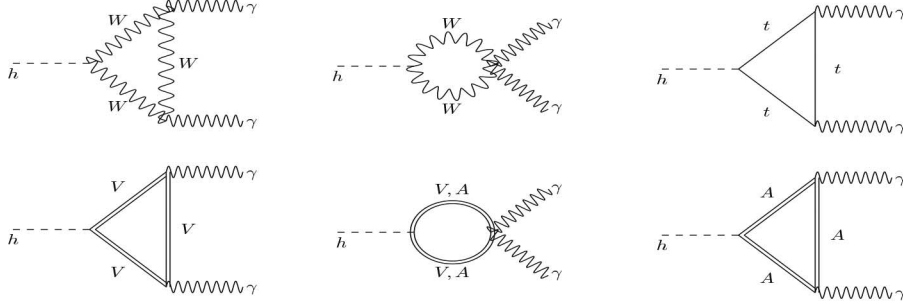


Fig. 1. – One-loop Feynman diagrams in the Unitary Gauge contributing to the  $h \rightarrow \gamma\gamma$  decay.

the LHC. To this end, we will introduce the ratio  $R_{\gamma\gamma}$ , which measures the  $\gamma\gamma$  signal produced in our model relative to the signal within the SM:

$$(2) \quad R_{\gamma\gamma} = \frac{\sigma(pp \rightarrow h)\Gamma(h \rightarrow \gamma\gamma)}{\sigma(pp \rightarrow h)_{SM}\Gamma(h \rightarrow \gamma\gamma)_{SM}} \simeq a_{htt}^2 \frac{\Gamma(h \rightarrow \gamma\gamma)}{\Gamma(h \rightarrow \gamma\gamma)_{SM}},$$

where  $a_{htt}$  is the deviation of the Higgs-top quark coupling with respect to the SM. Let us first study the  $\kappa$  dependence ( $\kappa = M_V^2/M_A^2$ ) of the two-photon signal, given in terms of the ratio  $R_{\gamma\gamma}$  of eq. (2), trying to find values in the range  $R_{\gamma\gamma} \sim 1$ –2. We should recall that  $M_V = g_C v/\sqrt{1-\kappa}$ . In fig. 2 we show  $R_{\gamma\gamma}$  as a function of  $\kappa$ , for a fixed value  $g_C v = 0.8$  TeV. As shown in fig. 2,  $R_{\gamma\gamma} \approx 1.7$  is obtained for  $\kappa \approx 0.078$  and  $0.71$ , which means a ratio  $M_V/M_A$  close to 0.28 or 0.84, respectively, in order to explain the excess of events in the  $h \rightarrow \gamma\gamma$  decay recently observed at the LHC. In a looser way, in order to get  $1 \lesssim R_{\gamma\gamma} \lesssim 2$  we find that  $\kappa$  has to be in the range  $0.061 \leq \kappa \leq 0.084$  or  $0.70 \leq \kappa \leq 0.73$ . The range  $0.1 < \kappa < 0.7$  is excluded because in this range  $\frac{a_{htt}^2}{4\pi} \gg 1$

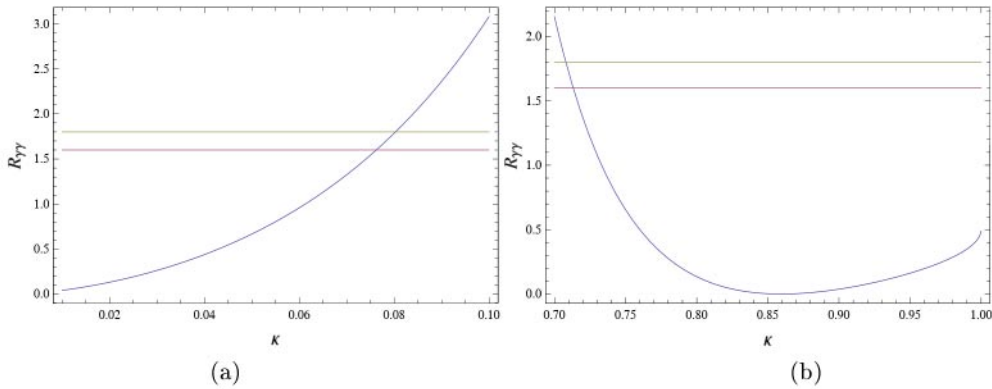


Fig. 2. – The ratio  $R_{\gamma\gamma}$  as a function of  $\kappa$  for  $g_C v = 0.8$  TeV. The horizontal lines are the  $R_{\gamma\gamma}$  experimental values given by CMS and ATLAS, which are equal to  $1.6 \pm 0.4$  and  $1.8 \pm_{0.419}^{0.460}$ , respectively [23, 24].

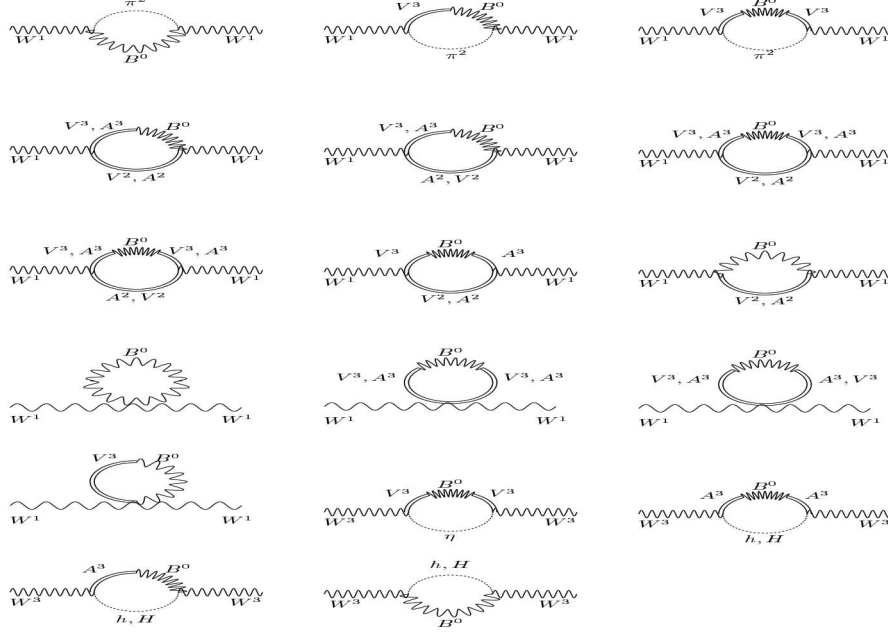


Fig. 3. – One-loop Feynman diagrams contributing to the  $T$  parameter.

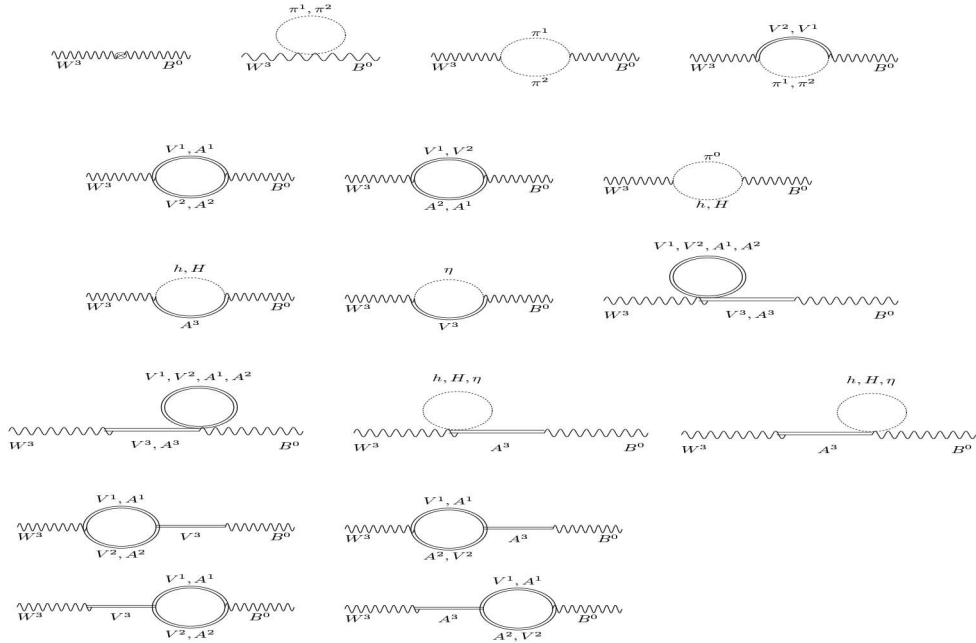


Fig. 4. – One-loop Feynman diagrams contributing to the  $S$  parameter.

and  $R_{\gamma\gamma}$  gets unacceptably large values. In that range, the one-loop computation of  $R_{\gamma\gamma}$  becomes unreliable. Let us now analyze the constraints imposed on the parameters by the values of  $T$  and  $S$  given by the experimental high precision tests of electroweak interactions. The Feynmann diagrams contributing to the  $T$  and  $S$  parameters are shown in figs. 3 and 4, respectively. Since  $T$  and  $S$  happen to have a rather mild sensitivity to the masses of  $H$  and  $\eta$ , and so we will restrict our study to a scenario where  $H$  and  $\eta$  are degenerate in mass at a value of 1 TeV. In contrast, most of the other diagrams, *i.e.* those containing SM bosons and/or the composite spin-1 fields  $V_\mu$  or  $A_\mu$ , have quartic and quadratic dependence on the cutoff, and as a consequence they are very sensitive to the masses  $M_V$  and  $M_A$ . We can separate the contributions to  $T$  and  $S$  as  $T = T_{SM} + \Delta T$  and  $S = S_{SM} + \Delta S$ , where

$$(3) \quad T_{SM} = -\frac{3}{16\pi \cos^2 \theta_W}, \quad S_{SM} = \frac{1}{12\pi} \ln \left( \frac{m_h^2}{m_W^2} \right)$$

are the contributions within the SM, while  $\Delta T$  and  $\Delta S$  contain all the contributions involving the extra particles. Then, the experimental results on  $T$  and  $S$  impose the restriction that  $\Delta T$  and  $\Delta S$  must lie inside a region in the  $\Delta S$ - $\Delta T$  plane. Explicitly, the experimentally allowed region at the 95% CL in the  $\Delta S$ - $\Delta T$  plane is the ellipse shown in figs. 5. In order to have  $\Delta T$  inside that region, we find that  $M_A$  should have a value in the range 1.76 TeV–2.15 TeV and  $M_V \simeq 0.84M_A$ , in order to satisfy these constraints, and at the same time yield a  $h \rightarrow \gamma\gamma$  signal near the recent experimental observations at the LHC. For numerical purposes, we then proceed to select a few representative discrete values of the axial vector mass  $M_A$ , namely 1.76 TeV, 1.9 TeV and 2.15 TeV, and then compute the resulting  $T$  and  $S$  parameters. Accordingly, for the three chosen cases, namely  $M_A = 1.76$  TeV, 1.9 TeV and 2.15 TeV, we find that the corresponding values of  $M_V$  must be 1.48 TeV, 1.6 TeV and 1.81 TeV in order to have an excess of events in the  $h \rightarrow \gamma\gamma$  decay  $R_{\gamma\gamma} \simeq 1.7$ . Note that we have discarded the case  $M_V/M_A \sim 0.28$ , which also gives  $R_{\gamma\gamma} \simeq 1.7$  (see fig. 2(a)), since in that case  $\Delta T$  falls outside the experimental bounds.

Now, continuing with the analysis of the constraints in the  $\Delta T$ - $\Delta S$  plane, we also find that, in order to fulfill the constraint on  $\Delta S$  as well, an additional condition must be met: for the aforementioned range of values of  $M_V$  and  $M_A$ , the  $S$  parameter turns out to be unacceptably large, unless a modified  $W^3 - B^0$  mixing is added. Here we introduce this mixing in terms of a coupling  $c_{WB}$  (see eq. (1)).

As is shown in figs. 5, we find that the coupling  $c_{WB}$  should be in the ranges  $0.233 \leq c_{WB} \leq 0.235$ ,  $0.186 \leq c_{WB} \leq 0.189$  and  $0.132 \leq c_{WB} \leq 0.133$  for the cases  $M_A = 1.76$  TeV, 1.9 TeV and 2.15 TeV, respectively. In figs. 5(a), (b) and (c) we show the allowed regions for the  $\Delta T$  and  $\Delta S$  parameters, for three different sets of values of  $M_V$  and  $M_A$ . The ellipses denote the experimentally allowed region at 95% CL, while the horizontal line shows the values of  $\Delta T$  and  $\Delta S$  in the model, as the mixing parameter  $c_{WB}$  is varied over the specified range in each case. As shown,  $\Delta T$  does not depend on  $c_{WB}$  (*i.e.* the line is horizontal), while  $\Delta S$  does. Moreover, the ranges for  $c_{WB}$  clearly exclude the case  $c_{WB} = 0$ , as  $\Delta S$  would fall outside the allowed region (the point would be further to the left of the corresponding ellipse).

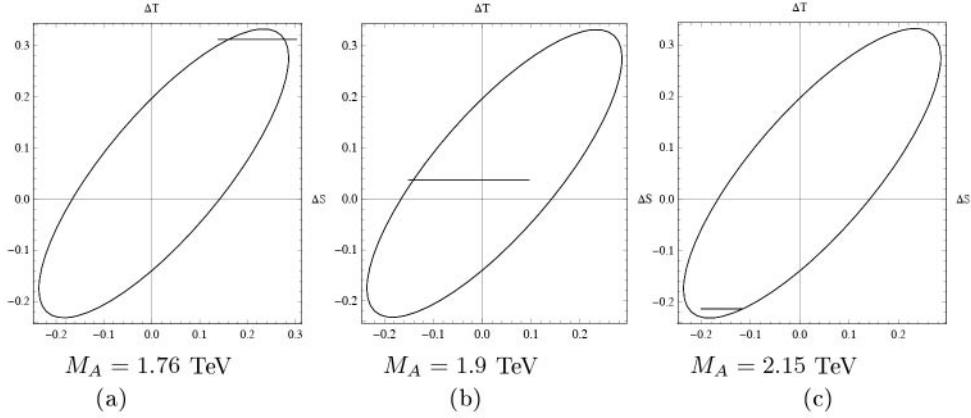


Fig. 5. – The  $\Delta S$ - $\Delta T$  plane in our model with composite scalars and vector fields. The ellipses denote the experimentally allowed region at 95% CL taken from [25]. The origin  $\Delta S = \Delta T = 0$  corresponds to the Standard Model value, with  $m_h = 125.7$  GeV and  $m_t = 176$  GeV. Panels (a), (b) and (c) correspond to three different sets of values for the masses  $M_A$ , as indicated with  $\kappa \simeq 0.71$ . The horizontal line shows the values of  $\Delta S$  and  $\Delta T$  in the model, as the mixing parameter  $c_{WB}$  varies over the ranges  $0.233 \leq c_{WB} \leq 0.235$  (a),  $0.186 \leq c_{WB} \leq 0.189$  (b), and  $0.132 \leq c_{WB} \leq 0.133$  (c).

#### 4. – Conclusions

We considered a framework of electroweak symmetry breaking without fundamental scalars, based on an underlying dynamics that becomes strong at a scale which we assume  $\Lambda \sim 3$  TeV. In general, below this scale there could be composite fields, bound by the strong dynamics. The spectrum of composite fields with masses below that scale is assumed to consist of spin-zero and spin-one fields, and the interactions among these particles and those of the Standard Model can be described by a  $SU(2)_L \times SU(2)_R / SU(2)_{L+R}$  effective chiral Lagrangian. Specifically, the composite fields included here are two scalars,  $h$  and  $H$ , one pseudoscalar  $\eta$ , a vector triplet  $V_\mu^a$  and an axial vector triplet  $A_\mu^a$ . The lightest scalar,  $h$ , is taken to be the newly discovered state at the LHC, with mass near 126 GeV. We will also assume that only  $h$  couples directly to the SM fermions, but  $H$  and  $\eta$  do not. In this scenario, in general one must include a deviation of the Higgs-fermion coupling with respect to the SM, which is parametrized here in terms of a coupling we call  $a_{hff}$ . This coupling is constrained from the requirement of good asymptotic behavior for the scattering of two longitudinal SM gauge bosons into a SM fermion pair. Our main goal within this framework is to study the effect of the composite particles in the decay  $h \rightarrow \gamma\gamma$ . We found this rate to be consistent with the LHC observations provided the ratio between the composite vector and axial vector masses falls in a narrow range  $M_V/M_A \sim 0.84$ . We found that the constraints on the  $T$  parameter at 95% CL, together with the previously mentioned requirement of the  $h \rightarrow \gamma\gamma$  decay rate, restrict the axial vector masses to be in the range  $1.76 \text{ TeV} \lesssim M_A \lesssim 2.15 \text{ TeV}$ . In addition, consistency with the experimental value on the  $S$  parameter requires the presence of a modified  $W^3 - B^0$  mixing, which we parametrize in terms of a coupling  $c_{WB}$ .

\* \* \*

This work was supported in part by Conicyt (Chile) grant ACT-119 “Institute for advanced studies in Science and Technology”. C.D. also received support from Fondecyt (Chile) grant No. 1130617, and A.Z. from Fondecyt grant No. 1120346 and Conicyt grant ACT-91 “Southern Theoretical Physics Laboratory”. A. E. C. H. thanks the organizers of the “Les Rencontres de Physique de la Vallée d’Aoste”, especially Professor Gino Isidori for inviting him to present this talk.

## REFERENCES

- [1] AAD G. *et al.* (THE ATLAS COLLABORATION), *Phys. Lett. B*, **716** (2012) 1.
- [2] CHATRCHYAN S. *et al.* (THE CMS COLLABORATION), *Phys. Lett. B*, **716** (2012) 30.
- [3] AALTONEN T. *et al.* (CDF and D0 COLLABORATIONS), *Phys. Rev. Lett*, **109** (2012) 071804.
- [4] BERINGER J. *et al.* (PARTICLE DATA GROUP), *Phys. Rev. D*, **86** (2012) 010001.
- [5] KAPLAN D. B. and GEORGI H., *Phys. Lett. B*, **136** (1984) 183.
- [6] CHIVUKULA R. S. and KOULOVASSILOPOULOS V., *Phys. Lett. B*, **309** (1993) 371.
- [7] GIUDICE G. F., GROJEAN C., POMAROL A. and RATTAZZI R., *JHEP*, **06** (2007) 045.
- [8] BARBIERI R., BELLAZINI B., RYCHKOV V. S. and VARAGNOLO A., *Phys. Rev. D*, **76** (2007) 115008.
- [9] ANASTASIOU C., FURLAN E. and SANTIAGO J., *Phys. Rev. D*, **79** (2009) 075003.
- [10] MARZOCCA D., SERONE M. and SHU J., *JHEP*, **08** (2012) 013.
- [11] POMAROL A. and RIVA F., *JHEP*, **08** (2012) 135.
- [12] BARBIERI R., BUTTAZZO D., SALA F., STRAUB D. and TESI A., *JHEP*, **05** (2013) 069.
- [13] CASALBUONI R., DEANDREA A., CURTIS S. DE., DOMINICI D., GATTO R. and GRAZZINI M., *Phys. Rev. D*, **53** (1996) 5201.
- [14] BARBIERI R., ISIDORI G., RYCHKOV V. S. and TRINCHERINI E., *Phys. Rev. D*, **78** (2008) 036012.
- [15] BARBIERI R., CÁRCAMO HERNÁNDEZ A. E., CORCELLA G., TORRE R. and TRINCHERINI E., *JHEP*, **03** (2010) 068.
- [16] CASALBUONI R., CURTIS S. DE., DOMINICI D. and GATTO R., *Nucl. Phys. B*, **282** (1987) 235.
- [17] CÁRCAMO HERNÁNDEZ A. E. and TORRE R., *Nucl. Phys. B*, **841** (2010) 188.
- [18] BELLAZINI B., CSAKI C., HUBISZ J., SERRA J. and TERNING J., *JHEP*, **11** (2012) 003.
- [19] CONTINO R., MARZOCCA D., PAPPADOPULO D. and RATTAZZI R., *JHEP*, **10** (2011) 081.
- [20] CÁRCAMO HERNÁNDEZ A. E., DIB C. O. and ZERWEKH ALFONSO R., hep-ph/1304.0286, preprint (2013).
- [21] KAPLAN D. B., *Nucl. Phys. B*, **365** (1991) 259.
- [22] BARBIERI R., ISIDORI G. and PAPPADOPULO D., *JHEP*, **02** (2009) 029.
- [23] CERN Report No. ATLAS-CONF-2012-170, 2012 (unpublished).
- [24] CERN Report No. CMS-PAS-HIG-12-045, 2012 (unpublished).
- [25] BAAK M. *et al.*, *Eur. Phys. J. C*, **72** (2012) 2003.